Mechanism of protein binding to spherical polyelectrolyte brushes studied *in situ* using two-photon excitation fluorescence fluctuation spectroscopy

C. Czeslik* and R. Jansen
Physikalische Chemie I, Universität Dortmund, D-44221 Dortmund, Germany

M. Ballauff* and A. Wittemann
Polymer-Institut, Universität Karlsruhe, D-76128 Karlsruhe, Germany

C. A. Royer
Centre de Biochimie Structurale, INSERM, F-34090 Montpellier, France

E. Gratton and T. Hazlett
Laboratory for Fluorescence Dynamics, University of Illinois, Urbana, Illinois 61801, USA
(Received 8 September 2003; published 19 February 2004)

We used two-photon excitation fluorescence fluctuation spectroscopy with photon counting histogram (PCH) analysis as a new tool to study the binding of globular proteins to colloidal particles *in situ*. Whereas fluorescence fluctuations are traditionally evaluated by calculating the autocorrelation function (fluorescence correlation spectroscopy), a complementary PCH analysis has been performed in this study which is advantageous when particle concentrations of a multicomponent system are of interest and the particles can be distinguished through particle brightness differences. The binding of two proteins, staphylococcal nuclease (SNase) and bovine serum albumin (BSA), to spherical polyelectrolyte brushes (SPB) was measured as a function of protein concentration and ionic strength of the solution at pH-values where SNase and BSA are positively and negatively charged, respectively. It has been found that SNase and BSA strongly bind to the SPB regardless of the protein charge. When the ionic strength of the solution is raised to 100 mM, the SPB become resistant to both proteins. These findings provide further evidence for a binding mechanism where the proteins are mainly driven to the SPB by the ''counterion evaporation'' force, while Coulomb interactions play a minor role. The results of this study characterize the potential of SPB as a new class of carrier particles for proteins whose use in biotechnological applications appears to be rewarding.

DOI: 10.1103/PhysRevE.69.021401 PACS number(s): 82.70.Dd, 87.15.Kg

I. INTRODUCTION

The development and investigation of biofunctional nanoparticles consisting of protein (enzyme) molecules immobilized on colloidal carrier particles is currently a very active research field [1–11]. These bionanoparticles are characterized by a high local density of protein molecules and may be used in the fields of biomedicine and biotechnology as drug delivery systems, biosensors, immunoassays, and biocatalysts.

To design bionanoparticles, the protein molecules may be adsorbed directly on hard colloidal particles, such as silica or poly(styrene) particles. Although the biological activity of the proteins is preserved in some cases, significant changes in the secondary structure of the protein molecules are often observed due to the interaction of the protein with the solid surface of the particles [12–14]. Furthermore, upon adsorption to solid surfaces, the internal dynamics of enzymes may be reduced, leading to poor catalytic activity [15]. In a series of studies, polyelectrolyte layers have been found to be a favorable immobilizing substrate for proteins, since the native conformation of the protein molecules appears largely preserved, protein-protein aggregation can be prevented, and the activity of enzymes remains high when the protein molecules are in contact with these layers [1,2,11,16,17]. Bionanoparticles coated with polyelectrolyte layers are generally prepared using the layer-by-layer deposition method where polyelectrolytes of opposite charges are deposited on core particles [1,2,18]. Protein molecules are adsorbed on the particles in the last step or are embedded between polyelectrolyte layers.

Recently, spherical polyelectrolyte brushes (SPBs) have been presented as a new class of carrier particles for proteins [19]. The SPBs consist of a solid core of poly(styrene) onto which long linear polyelectrolyte chains of poly(acrylic acid) (PAA) or poly(styrene sulfonic acid) (PSS) are grafted [20–22]. Because of their colloidal size and their brush structure these particles exhibit a large interfacial area in solution that is well defined and able to bind large amounts of protein. Indeed, SPBs with PAA chains have been found to strongly bind bovine serum albumin (BSA) at a low ionic strength [19]. In addition to a high protein binding capacity, SPBs provide a mild environment for protein molecules, since the conformation and the enzymatic activity of adsorbed proteins have been found to be largely preserved [23,24].

To study the degree of protein adsorption at planar aqueous/solid interfaces a series of reflectometric techniques can be applied [25,26]. In the case of colloidal particle surfaces, the degree of protein binding has primarily been ob-

*Corresponding author.

tained indirectly using the depletion method [27]. Here, we introduce the use of two-photon excitation fluorescence fluctuation spectroscopy with photon counting histogram (PCH) analysis as a new method to study the binding of proteins to colloidal particles *in situ*. This approach allows a miniaturization of the sample volume, as compared to other techniques, and reports on the concentration and the fluorescence brightness of the diffusing species [28,29]. Traditionally, fluorescence fluctuation time series are analyzed by evaluating the autocorrelation function, i.e., fluorescence correlation spectroscopy (FCS) is applied [30,31]. Complementary, the PCH can also be calculated from the fluorescence fluctuation data. As shown here, PCH analysis is superior to FCS when the concentrations of multiple species are to be determined, and the various species show differences in their brightnesses but only minor differences in their diffusion times.

In a previous study, the amount of BSA adsorbed to SPB was measured *ex situ*, i.e., in the absence of free, nonadsorbed protein. Weakly and nonadsorbed BSA was removed from a BSA/SPB suspension by ultrafiltration, and the protein concentration of the filtrate was determined using ultraviolet spectroscopy [19]. The aim of this study was to characterize the binding of globular proteins to SPBs *in situ*, thereby presenting fluorescence fluctuation spectroscopy with PCH analysis as a new tool for the investigation of protein/colloid systems. BSA and staphylococcal nuclease (SNase) were selected as model proteins. BSA is characterized by an isoelectric point at pH$=5$ and is composed of 582 amino acid residues [32], whereas SNase has 149 amino acid residues and an isoelectric point at pH$=9.5$. At neutral pH values, BSA and SNase are negatively and positively charged, respectively. Thus, the effects of protein size and net charge on the degree of binding to the SPB can be investigated and compared.

BSA, with a net negative charge, is adsorbed to a SPB at low ionic strength and can be desorbed from the SPB by rinsing with a 500-mM sodium chloride solution [19]. This finding is somewhat surprising, since one would expect that the elevated ionic strength should lead to a decreased electrostatic repulsion between the BSA and the SPB and thus to an enhanced protein binding. For example, when negatively charged BSA adsorbs on negatively charged planar surfaces composed of poly(styrene sulfonic acid) or silica, enhanced adsorption is observed at higher ionic strength only [33,34]. As will be shown in this study, the mechanism of protein binding to SPBs is mainly based on a release of small counterions of the SPB. The dominance of this entropic driving force has not been observed before for other protein/colloid systems.

II. EXPERIMENT

Staphylococcal nuclease was obtained as described before [35]. Bovine serum albumin was purchased from Sigma (catalog number A-6003). Both proteins were analyzed by gel electrophoresis and were found to be essentially pure ($>99\%$). SNase was labeled with fluorescein by adding fluorescein-isothiocyanate (Molecular Probes) to a solution of SNase in carbonate buffer (100 mM, pH$=7.9$). After about 45 min, unbound dye molecules were separated from the solution using a Sephadex G-25 column which was rinsed with a morpholinopropanesulfonic acid (MOPS) buffer (10 mM, pH$=7.0$). From ultraviolet (UV) spectroscopy of the purified stock solution, a degree of labeling of 21% and an SNase concentration of 13.7 μM were determined. BSA was labeled with Texas Red dye (Molecular Probes) by adding the dye to BSA dissolved in carbonate buffer (100 mM, pH$=8.4$). After about 60 min, unbound dye molecules were removed from the BSA solution using a Sephadex G-25 column which was rinsed with a morpholinoethanesulfonic acid (MES) buffer (10 mM, pH$=6.1$). From UV spectroscopy of the purified stock solution, a degree of labeling of 91% and a BSA concentration of 1.1 μM were determined.

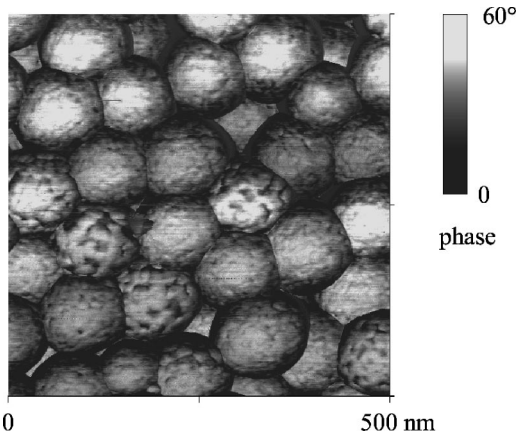

FIG. 1. Atomic force microscopy image of spherical polyelectrolyte brushes (SPB) with poly(acrylic acid) chains. The image was recorded in tapping mode at the air and displays the phase of the oscillating cantilever tip.

The spherical polyelectrolyte brushes that serve as substrate for SNase and BSA in this study consist of a poly(styrene) (PS) core and a poly(acrylic acid) shell. They were prepared by photoemulsion polymerization as described before [22]. The radius of the PS core is 51 nm, the contour length of the PAA chains is 36 nm and the grafting density is 0.13 nm^{-2}. To get a visual impression of the SPB, an atomic force microscopy image of the SPB is shown in Fig. 1. It was obtained by spreading an aqueous solution of the SPB on a freshly cleaved mica surface. After drying, the image was recorded in the tapping mode using the Multimode atomic force microscope (AFM) from Digital Instruments. The image illustrates the homogeneous size of the particles. Some neighboring particles share straight borders which indicates a compression or an interdigitation of the polyelectrolyte brushes of the particles. Particle diameters of 100 ± 5 nm are measured when the brush is compressed, whereas particles without neighbors show diameters of about 129 nm. A detailed AFM study of SPBs can be found elsewhere [36].

The following systems have been characterized in this study by fluorescence fluctuation spectroscopy: SNase/SPB/NaCl in a MOPS buffer (10 mM, pH$=7.0$) and BSA/SPB/NaCl in a MES buffer (10 mM, pH$=6.1$) at varying concentrations of the protein and sodium chloride. SPB stock solutions of 1 $\mu g/\mu L$ in a MOPS or MES buffer were prepared. Then, appropriate amounts of the protein and the SPB stock solutions were added to buffer solutions containing dif-

ferent concentrations of sodium chloride. After intensive mixing, the samples were equilibrated for at least 1 h before the measurement.

The two-photon excitation fluorescence fluctuation measurements were carried out at the Laboratory for Fluorescence Dynamics (LFD) at the University of Illinois (Urbana, Illinois, USA). A Zeiss Axiovert 135 TV inverted microscope with a Zeiss F Fluar 40×/1.30 oil objective was used. The excitation light source was a Coherent Mira 900 mode-locked Ti:sapphire laser which was pumped by a Coherent Verdi cw laser (532 nm, 5 W). The excitation light had a wavelength of 780 nm, a pulse frequency of 80 MHz and a pulse width of about 150 fs at the sample. An avalanche photodiode (EG&G, model SPCM-AQR-15) was used as the fluorescence detector. The output of the photodiode was directly read into a home-built (LFD) computer acquisition card and stored in memory. The photon counts were sampled at 20 kHz. Data were processed and analyzed with SimFCS and Globals Unlimited™ software packages developed at the LFD. A three-dimensional Gaussian point spread function was assumed which was calibrated using an 11 nM fluorescein solution at pH>9 (the diffusion constant is 300 $\mu m^2 s^{-1}$). All experiments were performed at least twice. The reproducibility of the experiments is given in the figures as error bars.

III. PCH AND FCS ANALYSIS

The observed fluorescence fluctuations emitted from the protein/SPB samples have been processed by calculating both autocorrelation curves (fluorescence correlation spectroscopy, FCS) and photon counting histograms. An autocorrelation function is given as [30,37]

$$G(\tau)=\frac{\langle \delta F(t)\cdot \delta F(t+\tau)\rangle}{\langle F(t)\rangle^2}, \tag{1}$$

where $\delta F(t)=F(t)-\langle F(t)\rangle$ is the fluorescence fluctuation at time t, given as the deviation of the fluorescence intensity $F(t)$ from the time-average $\langle F(t)\rangle$. If the fluorescence fluctuations are caused by diffusion of the fluorescent molecules into and out of the two-photon excitation volume, $G(\tau)$ can be described as

$$G(\tau)=\frac{\gamma}{\overline{N}}\cdot\frac{1}{1+8D\tau/r_0^2}\cdot\frac{1}{(1+8D\tau/\omega_0^2 r_0^2)^{1/2}}, \tag{2}$$

where γ is a geometric factor depending on the shape of the excitation volume [38], $\overline{N}$ is the mean number of fluorescent molecules within the excitation volume, $\omega_0=z_0/r_0$ is the ratio of the excitation volume dimensions parallel and perpendicular to the beam axis, and D is the diffusion constant. For a two-component system, $G(\tau)$ is the sum of the individual autocorrelation functions weighted by the corresponding fractional intensities squared:

$$G(\tau)=\left(\frac{\varepsilon_1 N_1}{\varepsilon_1 N_1+\varepsilon_2 N_2}\right)^2\frac{\gamma}{N_1}g_1(\tau)+\left(\frac{\varepsilon_2 N_2}{\varepsilon_1 N_1+\varepsilon_2 N_2}\right)^2\frac{\gamma}{N_2}g_2(\tau), \tag{3}$$

where $g_i(\tau)=(1+8D_i\tau/r_0^2)^{-1}(1+8D_i\tau/\omega_0^2 r_0^2)^{-1/2}$ and ε_i is the molecular brightness of species i (number of photon counts per sampling time and molecule).

A photon counting histogram represents the probability to detect k photons per sampling time [28,29]. Whereas the autocorrelation function is determined by the average number of particles in the excitation volume $\overline{N}$ and their diffusion constant D, a PCH analysis yields $\overline{N}$ and the particle brightness ε. Briefly, the probability $p(k)$ to detect k photons from a single diffusing molecule is a weighted average of Poisson distributions, each with the mean value $\varepsilon I(\vec{r})$:

$$p(k)=\int\frac{[\varepsilon I(\vec{r})]^k\exp[-\varepsilon I(\vec{r})]}{k!}q(\vec{r})d\vec{r}, \tag{4}$$

where $I(\vec{r})$ is the point spread function normalized at the origin and $q(\vec{r})$ is the probability to find the molecule at position $\vec{r}$. To generalize this equation for N diffusing molecules, $I(\vec{r})$ and $q(\vec{r})$ must be replaced by $\Sigma_{i=1}^{N}I(\vec{r}_i)$ and $\Pi_{i=1}^{N}q(\vec{r}_i)$, respectively, and the integration is performed over the $3N$ coordinates of the molecules. Finally, to determine the PCH for an open two-photon excitation volume with a fluctuating number of molecules inside, we have to average $p(k)$ with a Poisson distribution $n(N)$ for the number of molecules:

$$\Pi(k)=\sum_{N=0}^{\infty}p(k)n(N). \tag{5}$$

The autocorrelation function of a multicomponent system can be decomposed, if the components have markedly different diffusion constants. However, a straightforward determination of the average particle numbers of the components is not possible, since these numbers are linked to the fractional intensities [Eq. (3)]. To extract particle numbers from the amplitude of an autocorrelation curve, the brightness of each component must be known or, in the case of a two-component system, at least the brightness ratio. In contrast, in a multicomponent analysis of a PCH, the average particle number and the brightness of each component are direct fitting parameters. This is the main reason why a PCH analysis is advantageous over FCS when the concentrations of species involved in a binding process are of interest.

IV. RESULTS AND DISCUSSION

Binding of proteins to SPB

Figure 2 shows autocorrelation curves that were calculated from fluorescence fluctuations according to Eq. (1). The fluorescence fluctuations were recorded from samples containing 10 μg of SPB and an increasing mass of SNase in a 1.5-mL buffer solution. Similar data were obtained when

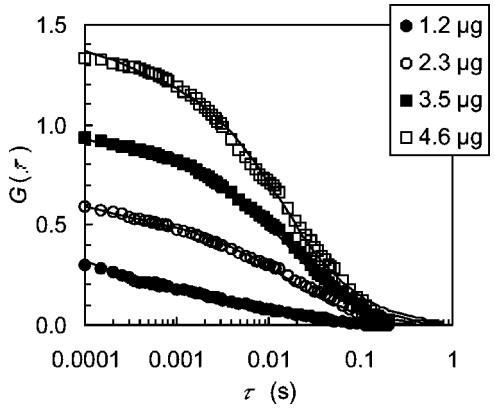

FIG. 2. Autocorrelation curves of the fluorescence fluctuations emitted from solutions contianing 10 μg of SPB and an increasing mass of SNase that is given in the inset. The symbols represent the experimental data, the solid lines show a global fit using a two-component model.

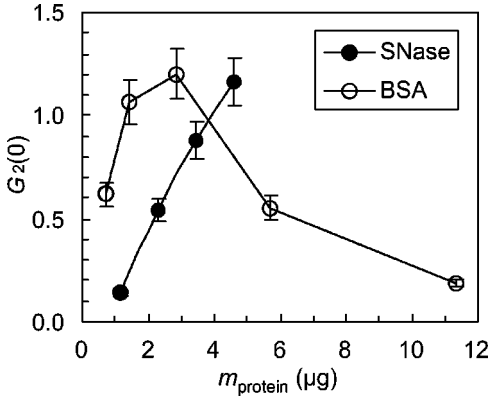

FIG. 3. Component amplitude of the slow diffusing SPB with adsorbed fluorescent protein molecules derived from the analysis of autocorrelation curves. The samples contained 10 μg of SPB and an increasing mass of protein in a 1.5-mL buffer solution.

BSA was added instead of SNase. As can be seen from this figure, the amplitude of the autocorrelation curves is increasing strongly with increasing protein mass. A two-component model was required to fit globally the autocorrelation curves (Fig. 2). In the global fitting procedure, the diffusion constant of the first component, D_1, was fixed to 110 $\mu m^2 s^{-1}$ for free SNase or to 60 $\mu m^2 s^{-1}$ for free BSA [39], whereas the diffusion constant of the second component, D_2, was varied but linked across the data set. This diffusion constant was found to be $D_2=(1.6\pm0.2)$ $\mu m^2 s^{-1}$ (for both SNase and BSA samples) and can thus be assigned to the slow diffusing SPBs with adsorbed fluorescent protein molecules. With a core radius of 51 nm and a shell thickness of 61 nm for the SPB [19], a diffusion constant of 1.9 $\mu m^2 s^{-1}$ can be calculated using the Stokes-Einstein relationship which is in good agreement with the experimental value. There was no effect of the adsorbed protein mass on the diffusion constant D_2, of the SPB which indicates that the size of the SPB is not significantly changing as protein molecules bind to the SPB. This result suggests that the protein molecules penetrate deeply into the polyelectrolyte brush shell, thereby leaving the overall dimension of the SPB unchanged. In the following text we continue to label the parameters of the free, nonadsorbed protein with index 1 and those of the protein-coated SPB with index 2.

In Fig. 3, the component amplitude $G_2(0)$ of the SPB with adsorbed fluorescent protein molecules is plotted as a function of the total protein mass in the samples as derived from the analysis of autocorrelation curves. The samples contained 10 μg of SPB and varying amounts of protein in a 1.5-mL buffer solution. In a simple model, the brightness of a single protein-coated spherical polyelectrolyte brush particle is proportional to the number of adsorbed protein molecules:

$$\varepsilon_2 = f\varepsilon_1 N_{ads}/N_2, \tag{6}$$

where ε_1 and ε_2 are the brightnesses of a nonadsorbed protein molecule and a protein-coated spherical polyelectrolyte brush particle, respectively, f reflects the change in brightness when a protein adsorbs on a brush, and N_{ads} and N_2 are the average numbers of adsorbed protein molecules and SPB particles in the observation volume, respectively. Then, according to Eq. (3), the component amplitude of the SPB can be written as

$$G_2(0) = \left(\frac{\varepsilon_2 N_2}{\varepsilon_1 N_1 + \varepsilon_2 N_2}\right)^2 \frac{\gamma}{N_2} = \frac{1}{[N_1/(N_{ads} f)+1]^2}\frac{\gamma}{N_2}, \tag{7}$$

where N_1 is the average number of non-adsorbed protein molecules in the observation volume. Thus, $G_2(0)$ can be regarded as a measure for the degree of protein binding to the SPB, since an increase of $G_2(0)$ corresponds to an increase of N_{ads}/N_1 (for constant values of N_2 and f). From the data plotted in Fig. 3, an increase of $G_2(0)$ is found when protein is added to the SPB which shows that the number of adsorbed protein molecules, N_{ads}, is increasing relative to the number of non-adsorbed protein molecules, N_1. This behavior is interesting, because it is contrary to that predicted by a Langmuir binding mechanism where N_{ads}/N_1 would always decrease when protein is added. Rather, the observed increase of N_{ads}/N_1 with increasing mass of protein is more consistent with a condensationlike binding where protein molecules are accumulated at the SPB while the number of nonadsorbed protein molecules remains low. In the case of BSA, a maximum is observed for $G_2(0)$ at a protein-SPB mass ratio of 3:10. At higher ratios, $G_2(0)$ is decreasing due to a limited protein binding capacity of the SPB that leads to an increase of N_1 relative to N_{ads} (this does not mean that BSA is desorbing from the SPB). A mass ratio of 3:10 corresponds to about 2000 BSA molecules adsorbed on a single spherical polyelectrolyte brush.

In Fig. 4, photon counting histograms are plotted that were determined from the same fluorescence fluctuations used for the calculation of the autocorrelation functions shown in Fig. 2. Thus, Figs. 2 and 4 are simply different, complementary representations of the same observed fluorescence fluctuations. The samples contained 10 μg of SPB

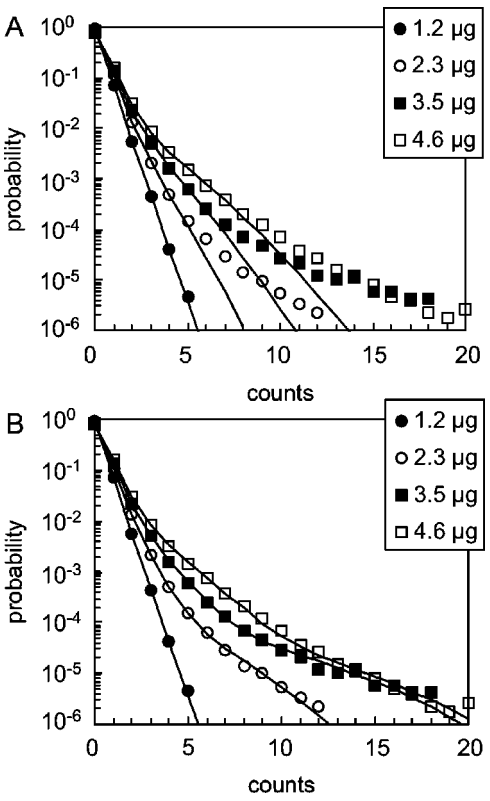

FIG. 4. Photon counting histograms of solutions containing 10 μg of SPB and an increasing mass of SNase that is given in the inset. The symbols represents the experimental data, the solid lines show global fits using a two-component model (A) and a three-component model (B).

with a variable mass of SNase in a 1.5-mL buffer solution. Very similar data were recorded when BSA was added instead of SNase. To analyze the data of Fig. 4, a two-component model was first used with average particle numbers N_1 and N_2 and brightnesses ε_1 and ε_2 as fitting parameters to represent the nonadsorbed protein molecules (index 1) and the SPB with adsorbed protein molecules (index 2). This two-component model was fitted globally to the data by fixing the protein brightness to $\varepsilon_1=0.923$ (SNase) or $\varepsilon_1=1.584$ (BSA) and by linking the particle number N_2 of the SPB across a data set. The protein brightnesses were determined before in separate experiments in the absence of a SPB. The average particle number of the SPB in the observation volume was found to be $N_2=0.015\pm0.002$. However, a satisfactory fit could not be obtained [Fig. 4(A)]. Therefore, to also sample the smaller probabilities, a three-component model was fitted globally to the PCH data by fixing ε_1 and N_2 to the values of the two-component model and by linking N_3 across a data set. With this model, the fit represents the photon counting histograms over more than five orders of magnitude [Fig. 4(B)]. The third component can be assigned to a small fraction of SPBs with a higher number of adsorbed protein molecules, since it was found that $N_3=0.0020\pm0.0008$ and $\varepsilon_3>\varepsilon_2$. For example, the PCH of a sample containing 10 μg of SPB and 4.6 μg of SNase yields values of $\varepsilon_1=0.923$, $\varepsilon_2=9.710$, $\varepsilon_3=22.875$, $N_1=0.110$, $N_2=0.016$, and $N_3=0.0012$. It is noted that the corresponding analysis of the autocorrelation functions (Fig. 2) cannot resolve the third component, since colloidal particles with different amounts of adsorbed protein differ in brightness but not significantly in their diffusion constant. Thus, $G_2(0)$, as given by Eq. (7), results from both SPB components. This reflects a known limitation of FCS in distinguishing particles with similar diffusion constants. PCH analysis, on the other hand, is based on differences in the magnitude and frequency of the fluorescence fluctuations and has been shown to resolve particles with a brightness ratio of two [40]. The existence of two SPB components with a low and a high number of adsorbed protein molecules may be interpreted as an indication for a distribution for the number of adsorbed protein molecules. We note that no indication has been observed for an aggregation of the SPB or a fluorescence quenching over time as judged from the analysis of repeated measurements and the time series of the fluorescence fluctuations.

To obtain the average number of adsorbed protein molecules per spherical polyelectrolyte brush as a function of the protein concentration in solution (i.e., the adsorption isotherm), a stepwise approach was taken. First, from the total number of SPBs in the observation volume ($N_{\mathrm{SPB}}=N_2+N_3$) and the known SPB bulk concentration, the size of the observation volume was calculated. Second, knowing the total bulk concentration of the protein, the average total number of protein molecules in the observation volume was determined. Third, since the number N_1 of free, nonadsorbed protein molecules in the observation volume is given by the global fit of the PCH data, the number of adsorbed protein molecules per spherical polyelectrolyte brush and the concentration of non-adsorbed protein molecules can be determined. Adsorption isotherms obtained in this way are plotted in Fig. 5 for both SNase and BSA. From these isotherms it can be seen that at a protein concentration of 0.5 nM about 10000 SNase and 2500 BSA molecules are adsorbed on a single spherical polyelectrolyte brush. Since SNase has a net positive charge and BSA has a net negative charge, it appears likely that electrostatic interactions between the protein molecules and the SPB are dominating. However, other parameters as the size of the protein molecules are also important (see below). It is noted that the adsorption isotherms shown in Fig. 5 reflect an almost quantitative binding of the proteins to the SPB. For example, at a protein concentration of 0.5 nM, more than 99.5% of all SNase molecules and about 98.7% of all BSA molecules are adsorbed at the SPB. For comparison, numbers of BSA molecules that remain adsorbed on a spherical polyelectrolyte brush after intensive washing with pure buffer solution are included in Fig. 5 (the data are taken from Ref. [19]). The difference between the *ex situ* data of Ref. [19] and the *in situ* data of this study is rather small. For example, if the degree of BSA binding to the SPB is slightly reduced from 98.7%, as measured *in situ* in this study, to 94.8% by washing with pure buffer solution, the fraction of nonadsorbed protein molecules increases from 1.3% to 5.2%. Thus, whereas the number of adsorbed BSA molecules is only slightly affected by washing, the protein concentration in solution is increased by a factor of four as observed (Fig. 5).

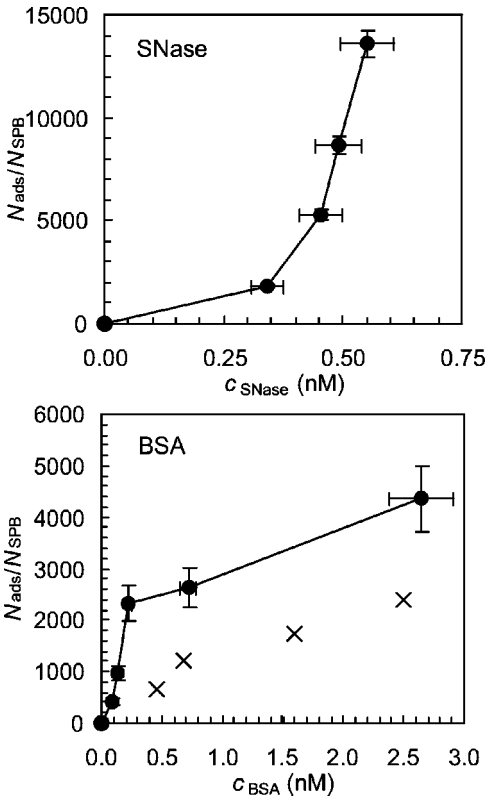

FIG. 5. Number of protein molecules adsorbed per spherical polyelectrolyte brush particle as a function of the protein concentration in solution ($N_{SPB}=N_2+N_3$). The data were derived from a PCH analysis of fluorescence fluctuations. For comparison, numbers of BSA molecules that remain adsorbed on a spherical polyelectrolyte brush after intensive washing with pure buffer solution are included as crosses (data taken from Ref. [19]).

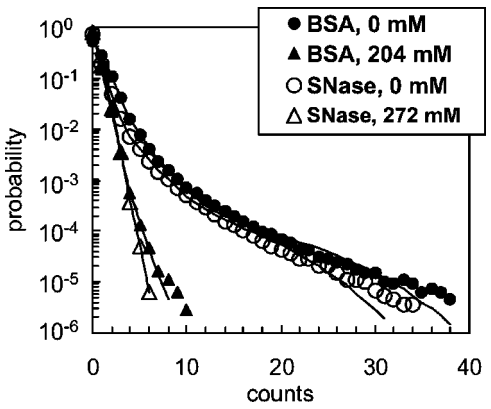

FIG. 6. Selected photon counting histograms of solutions containing 10 μg of SPB with 4.6-μg SNase or 20-μg SPB with 2.84-μg BSA at different concentrations of sodium chloride that is given in the inset. The chosen protein-SPB mass ratios correspond to an almost quantitative binding of the proteins to the SPB in the absence of sodium chloride. The symbols represent the experimental data, the solid lines show global fits using three-component models.

Salt-induced protein resistance of the SPB

In Fig. 6, selected photon counting histograms are shown which illustrate the drastic effect of sodium chloride on the degree of protein binding to the SPB. When no salt is added, the histograms include high counts with significant probability as can be seen from the long wings extending to high counts. On the other hand, in the presence of sodium chloride with a concentration of only a few 100 mM, the histograms of both SNase and BSA are limited over the range of 0–10 counts. The absence of higher counts is related to the absence of SPBs with a large number of adsorbed protein molecules. As described in the previous subsection, a three-component model was fitted to the photon counting histograms where again component 1 represents the non-adsorbed protein molecules and components 2 and 3 are the SPB with different amounts of adsorbed protein molecules.

The brightness of the SPB is solely due to the adsorbed protein molecules. For example, the mean brightness of samples containing 10 μg of SPB and 4.6 μg of SNase is reduced from 20.8 in the absence of sodium chloride to 2.6 at a NaCl concentration of 272 mM [the mean brightness is calculated as $(\varepsilon_2 N_2+\varepsilon_3 N_3)/(N_2+N_3)$]. For samples containing 20 μg of SPB and 2.84 μg of BSA, corresponding values of 18.6 at 0-mM NaCl and 1.9 at 204-mM NaCl are found (Fig. 6). These values demonstrate that there is a salt-induced protein resistance of the SPB regardless of the net protein charge. Knowing the mean brightness of the SPB, the number of adsorbed protein molecules per single spherical polyelectrolyte brush was calculated as a function of sodium chloride concentration using the following equation:

$$\frac{N_{ads}}{N_{SPB}}=\frac{1}{f\varepsilon_1}\cdot\frac{\varepsilon_2 N_2+\varepsilon_3 N_3}{N_2+N_3}, \tag{8}$$

where $N_{SPB}=N_2+N_3$. As shown above, the number of adsorbed protein molecules, N_{ads}, in the absence of salt can be well approximated by the total number of protein molecules in the observation volume, so that the factor f can be determined. Values of $f=0.010$ and 0.014 were found for fluorescein-labeled SNase and Texas Red-labeled BSA, respectively, which reflect that the adsorbed protein molecules are buried in the brush of the SPB and are strongly quenched after excitation. Since the values of ε_1, ε_2, ε_3, N_2, and N_3 are directly given by the PCH fits, the number of adsorbed protein molecules per spherical polyelectrolyte brush can be calculated using Eq. (8). This is plotted in Fig. 7 as a function of the sodium chloride concentration for both proteins. As can be clearly seen in this figure, the number of adsorbed protein molecules is reduced to about 10% by increasing the concentration of sodium chloride to only about 100 mM regardless of the protein charge. This result is remarkable, because protein resistance of the SPB can be induced at a relatively low ionic strength. In contrast, when adsorbing human serum albumin on flat layers of positively charged poly(allyl hydrochloride) or negatively charged poly(styrene sulfonic acid), the amount of adsorbed protein is nearly unchanged after rinsing with a 150-mM sodium chloride solution [41].

Driving forces for adsorption

At a high ionic strength, electrostatic interactions between the protein molecules and the SPB are screened. Thus, the

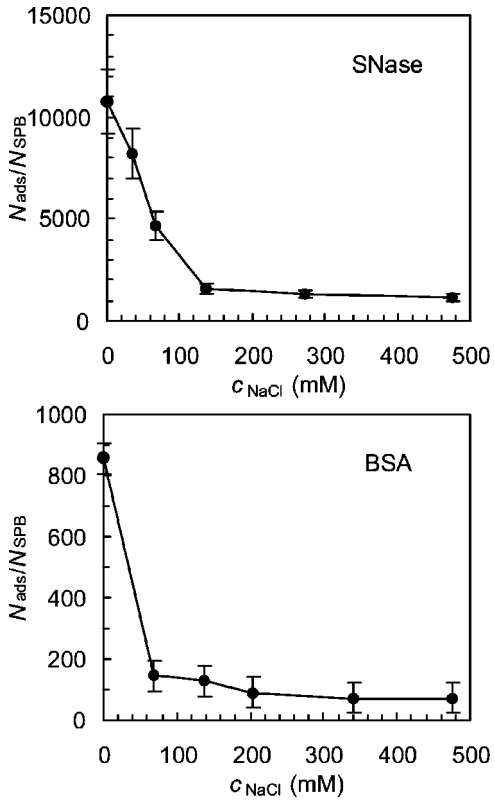

FIG. 7. Number of protein molecules adsorbed per spherical polyelectrolyte brush particle as a function of the concentration of sodium chloride ($N_{SPB}=N_2+N_3$). The data were derived from a PCH analysis of fluorescence fluctuations.

observed residual protein binding when the ionic strength in the solution is higher than about 200 mM (Fig. 7) must be attributed to some weak van der Waals or hydrophobic interactions between the protein molecules and the SPB. These types of interaction are generally believed to be responsible for protein adsorption at uncharged surfaces [42–44].

On the other hand, electrostatic interactions are important at low ionic strength where strong protein binding to the SPB is observed (Fig. 7). However, BSA has a net negative charge at pH=6.1, yet is binding strongly to the negatively charged SPB. As concluded in a recent study, this behavior can be attributed to attractive Coulomb forces between positively charged patches on the protein surface and the negatively charged SPB. These patches become multivalent counterions of the polyelectrolyte brush and a respective number of small ions is released [19]. This ''counterion evaporation'' increases the entropy of the system. These conclusions are strongly supported by the results of this study where the binding of the two proteins BSA and SNase to the SPB has been investigated *in situ*. Using model calculations, a counterion evaporation has also been shown to act as an entropic driving force for the adsorption of a polyelectrolyte chain at a charged surface [45].

To further illustrate the effect of SPB counterions on the degree of protein binding, the local ionic strength within the brush shell of the SPB has been calculated as a function of the sodium chloride concentration in the solution. According to Hariharan *et al.* [46], the local ionic strength within the

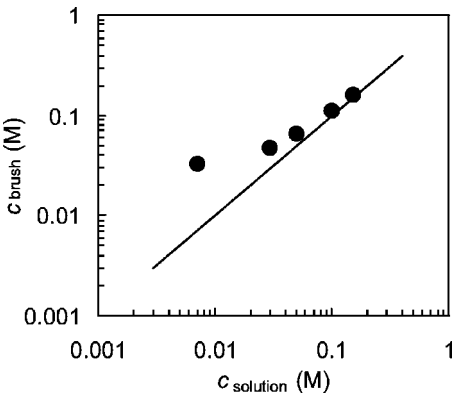

FIG. 8. Local ionic strength within the brush shell of the SPB as a function of the sodium chloride concentration in the bulk solution (solid circles). The data are calculated on the basis of the core radius and the shell thickness of the SPB taken from Ref. [19]. For comparison, the solid line shows $c_{brush}=c_{solution}$.

brush shell, c_{brush}, is given by

$$c_{brush}=\left[c_{solution}^2+\left(\frac{\rho}{2eN_A}\right)^2\right]^{1/2}, \tag{9}$$

where $c_{solution}$ is the sodium chloride solution concentration, e is the electron charge, and N_A is the Avogadro constant. The charge density ρ within the brush shell depends on the core radius R, the shell thickness L, and the grafting density σ of the SPB, as well as on the contour length L_c of the PAA chains and the Bjerrum length l_B:

$$\rho=\frac{3eR^2\sigma L_c}{l_B[(R+L)^3-R^3]}. \tag{10}$$

As can be seen from Fig. 8, the local ionic strength within the brush shell of the SPB is approaching the solution salt concentration in the concentration range of 10–100 mM. At salt concentrations greater than 100 mM, there is no difference between the salt concentrations of the surrounding and the SPB interior. Therefore, under these higher ionic strength conditions, counterion release cannot be the driving force for protein binding to the SPB. Indeed, we have observed a strongly reduced protein affinity for the SPB at these higher sodium chloride concentrations (Fig. 7). In addition, at higher salt concentrations, the polyelectrolyte brush of the SPB partially collapses and protein molecules are repelled from the SPB by steric interactions. At a low ionic strength, the dominance of a counterion release over other driving forces for protein binding to a SPB can be explained by the trapping of almost all counterions within the polyelectrolyte brush [47]. This quantitative confinement of counterions has not been found for nonbrush polyelectrolyte interfaces.

When comparing the numbers of adsorbed BSA and SNase molecules per single polyelectrolyte brush (Fig. 5), a higher number is found for SNase. Attractive Coulomb interactions between SNase and the SPB is a likely explanation for this finding. However, if one converts the numbers of adsorbed protein molecules to protein masses, both proteins show very similar binding, about 2.75×10^{-16}g BSA and

2.79×10^{-16}g SNase are adsorbed at protein solution concentrations of 0.5 nM. The similarity of the masses suggests that the protein binding capacity of the SPB is also determined by volume effects.

V. CONCLUSIONS

In this study, fluorescence fluctuation spectroscopy with PCH analysis has been presented as a new tool to investigate the binding of protein molecules to colloidal particles *in situ*. Whereas fluorescence fluctuations are traditionally processed by a calculation of the autocorrelation function, we have found that a complementary determination of the photon counting histogram (PCH) is advantageous when the particle numbers of a multicomponent system are of interest and the particles vary in their brightness. We have extended a recent report in which the degree of BSA binding to a SPB after intensive rinsing was studied [19]. In this work we report on the quantitative binding of two proteins, BSA (negatively charged) and SNase (positively charged), to SPBs *in situ*. Increasing the concentration of sodium chloride in the solution to approximately 100 mM leads to a drastically reduced protein affinity for the SPB. The results of this study provide further evidence for a counterion release as the almost single driving force for protein binding to SPBs. The dominance of this entropic driving force has not been reported so far for other protein/colloid systems.

ACKNOWLEDGMENTS

We thank the Deutsche Forschungsgemeinschaft (DFG) for financial support. The fluorescence experiments reported in this paper were performed at the Laboratory for Fluorescence Dynamics (LFD) at the University of Illinois at Urbana-Champaign (UIUC). The LFD is supported jointly by the National Center for Research Resources of the National Institutes of Health (PHS 5 P41-RRO3155) and UIUC.

[1] M. Fang, P. S. Grant, M. J. McShane, G. B. Sukhorukov, V. O. Golub, and Y. M. Lvov, Langmuir **18**, 6338 (2002).
[2] F. Caruso and C. Schüler, Langmuir **16**, 9595 (2000).
[3] F. Caruso and H. Möhwald, J. Am. Chem. Soc. **121**, 6039 (1999).
[4] E. Donath, G. B. Sukhorukov, F. Caruso, S. A. Davis, and H. Möhwald, Angew. Chem. **110**, 2323 (1998).
[5] F. Caruso, R. A. Caruso, and H. Möhwald, Science **282**, 1111 (1998).
[6] C. M. Niemeyer, Angew. Chem., Int. Ed. Engl. **40**, 4128 (2001).
[7] L. Yang and P. Alexandridis, Curr. Opin. Colloid Interface Sci. **5**, 132 (2000).
[8] J. L. Ortega-Vinuesa and R. Hidalgo-Alvarez, Biotechnol. Bioeng. **47**, 633 (1995).
[9] J. M. Peula, J. Puig, J. Serra, F. J. de las Nieves, and R. Hidalgo-Alvarez, Colloids Surf., A **92**, 127 (1994).
[10] J.-Y. Yoon, H.-Y. Park, J.-H. Kim, and W.-S. Kim, J. Colloid Interface Sci. **177**, 613 (1996).
[11] J. P. Santos, E. R. Welsh, B. P. Gaber, and A. Singh, Langmuir **17**, 5361 (2001).
[12] A. Kondo, F. Murakami, and K. Higashitani, Biotechnol. Prog. **40**, 889 (1992).
[13] W. Norde and J. P. Favier, Colloids Surf. **64**, 87 (1992).
[14] P. Billsten, M. Wahlgren, T. Arnebrant, J. McGuire, and H. Elwing, J. Colloid Interface Sci. **175**, 77 (1995).
[15] C. Czeslik, C. Royer, T. Hazlett, and W. Mantulin, Biophys. J. **84**, 2533 (2003).
[16] P. Schwinté, V. Ball, B. Szalontai, Y. Haikel, J.-C. Voegel, and P. Schaaf, Biomacromolecules **3**, 1135 (2002).
[17] P. Schwinté, J.-C. Voegel, C. Picart, Y. Haikel, P. Schaaf, and B. Szalontai, J. Phys. Chem. B **105**, 11906 (2001).
[18] G. Decher, Science **277**, 1232 (1997).
[19] A. Wittemann, B. Haupt, and M. Ballauff, Phys. Chem. Chem. Phys. **5**, 1671 (2003).
[20] X. Guo and M. Ballauff, Phys. Rev. E **64**, 051406 (2001).
[21] X. Guo and M. Ballauff, Langmuir **16**, 8719 (2000).
[22] X. Guo, A. Weiss, and M. Ballauff, Macromolecules **32**, 6043 (1999).
[23] G. Jackler, A. Wittemann, M. Ballauff, and C. Czeslik (unpublished).
[24] T. Neumann, B. Haupt, and M. Ballauff (unpublished).
[25] *Physical Chemistry of Biological Interfaces*, edited by A. Baszkin and W. Norde (Dekker, New York, 2000).
[26] *Biopolymers at Interfaces*, edited by M. Malmsten (Dekker, New York, 2003).
[27] C. A. Haynes, E. Sliwinsky, and W. Norde, J. Colloid Interface Sci. **164**, 394 (1994).
[28] Y. Chen, J. D. Müller, P. T. C. So, and E. Gratton, Biophys. J. **77**, 553 (1999).
[29] Y. Chen, J. D. Müller, K. M. Berland, and E. Gratton, Methods **19**, 234 (1999).
[30] S. T. Hess, S. Huang, A. A. Heikal, and W. W. Webb, Biochemistry **41**, 697 (2002).
[31] D. Magde, E. Elson, and W. W. Webb, Phys. Rev. Lett. **29**, 705 (1972).
[32] D. C. Carter and J. X. Ho, Adv. Protein Chem. **45**, 153 (1994).
[33] G. Ladam, P. Schaaf, G. Decher, J.-C. Voegel, and F. J. G. Cuisinier, Biomolec. Engineering **19**, 273 (2002).
[34] S. Robinson and P. A. Williams, Langmuir **18**, 8743 (2002).
[35] H. Seemann, R. Winter, and C. A. Royer, J. Mol. Biol. **307**, 1091 (2001).
[36] Y. Mei, A. Wittemann, G. Sharma, M. Ballauff, T. Koch, H. Gliemann, J. Horbach, and T. Schimmel, Macromolecules **36**, 3452 (2003).
[37] O. Krichevsky and G. Bonnet, Rep. Prog. Phys. **65**, 251 (2002).
[38] K. M. Berland, P. T. So, and E. Gratton, Biophys. J. **68**, 694 (1995).
[39] M. Placidi and S. Cannistraro, Europhys. Lett. **43**, 476 (1998).
[40] J. D. Müller, Y. Chen, and E. Gratton, Biophys. J. **78**, 474 (2000).

[41] G. Ladam, C. Gergely, B. Senger, G. Decher, J.-C. Voegel, P. Schaaf, and F. J. G. Cuisinier, Biomacromolecules **1**, 674 (2000).
[42] V. P. Zhdanov and B. Kasemo, Langmuir **17**, 5407 (2001).
[43] W. Norde, Macromol. Symp. **103**, 5 (1996).
[44] C. M. Roth and A. M. Lenhoff, Langmuir **11**, 3500 (1995).
[45] C. Fleck and H. H. von Grünberg, Phys. Rev. E **63**, 061804 (2001).
[46] R. Hariharan, C. Biver, and W. B. Russel, Macromolecules **31**, 7514 (1998).
[47] N. Dingenouts, R. Merkle, X. Guo, T. Narayanan, G. Goerigk, and M. Ballauff, J. Appl. Crystallogr. **36**, 578 (2003).